Molecules and Cells

Reduced EGFR Level in eIF2α Phosphorylation-Deficient Hepatocytes Is Responsible for Susceptibility to Oxidative Stress

Mi-Jeong Kim[1,3], Woo-Gyun Choi[1,3], Kyung-Ju Ahn[1], In Gyeong Chae[1], Rina Yu[2], and Sung Hoon Back[1,*]

[1]School of Biological Sciences and [2]Department of Food Science and Nutrition, University of Ulsan, Ulsan 44610, Korea, [3]These authors contributed equally to this work.
*Correspondence: shback@ulsan.ac.kr
https://doi.org/10.14348/molcells.2020.2197
www.molcells.org

Reactive oxygen species (ROS) play a significant role in intracellular signaling and regulation, particularly when they are maintained at physiologic levels. However, excess ROS can cause cell damage and induce cell death. We recently reported that eIF2α phosphorylation protects hepatocytes from oxidative stress and liver fibrosis induced by fructose metabolism. Here, we found that hepatocyte-specific eIF2α phosphorylation-deficient mice have significantly reduced expression of the epidermal growth factor receptor (EGFR) and altered EGFR-mediated signaling pathways. EGFR-mediated signaling pathways are important for cell proliferation, differentiation, and survival in many tissues and cell types. Therefore, we studied whether the reduced amount of EGFR is responsible for the eIF2α phosphorylation-deficient hepatocytes' vulnerability to oxidative stress. ROS such as hydrogen peroxide and superoxides induce both EGFR tyrosine phosphorylation and eIF2α phosphorylation. eIF2α phosphorylation-deficient primary hepatocytes, or EGFR knockdown cells, have decreased ROS scavenging ability compared to normal cells. Therefore, these cells are particularly susceptible to oxidative stress. However, overexpression of EGFR in these eIF2α phosphorylation-deficient primary hepatocytes increased ROS scavenging ability and alleviated ROS-mediated cell death. Therefore, we hypothesize that the reduced EGFR level in eIF2α phosphorylation-deficient hepatocytes is one of critical factors responsible for their susceptibility to oxidative stress.

Keywords: eIF2α phosphorylation, epidermal growth factor receptor, hydrogen peroxide, menadione, reactive oxygen species

INTRODUCTION

The epidermal growth factor receptor (EGFR), or ErbB1 receptor (ErbB1), is one of four members of the ErbB family of tyrosine kinase receptors. ErbB1 is expressed in various tissues and mediates cell proliferation, differentiation, migration and survival through various signaling pathways (Berasain and Avila, 2014). When a ligand such as epidermal growth factor (EGF) (Schneider and Wolf, 2009) binds to the EGFR, it forms homo- and hetero-dimers with all four family members (Berasain and Avila, 2014; Schneider and Wolf, 2009). Ligand-activated EGFR proteins are auto-phosphorylated and cross-phosphorylated at multiple tyrosine residues (such as Y1068), which are located in the C-terminal non-catalytic sequence (Sato, 2013). The autophosphorylated tyrosine residues are believed to serve as docking sites for a variety of signaling molecules (such as Src homology 2) that contain phosphotyrosine-binding domains (Carpenter and Cohen, 1990; Sato, 2013). Subsequently, the activated EGFR triggers

Received 28 August 2019; revised 17 December 2019; accepted 10 January 2020; published online 9 March, 2020

eISSN: 0219-1032

the following four main downstream signaling pathways: the PI3K/Akt pathway, the phospholipase C-gamma (PLC-γ)/protein kinase C (PKC) pathway, the ras/raf/MEK/MAPK pathway (comprised of the activation of extracellular signal-regulated kinase [ERK] and JUN N-terminal kinase [JNK]), and the signal transducers and activators of transcription (STATs) pathway (Citri and Yarden, 2006; Jorissen et al., 2003; Liebmann, 2011). The four signaling pathways collectively control cell proliferation, differentiation, migration, and survival.

Apart from ligand-dependent EGFR tyrosine activation, accumulating evidence has shown that reactive oxygen species (ROS) are involved in another mechanism of EGFR transactivation (Abdelmohsen et al., 2003; Chiarugi and Buricchi, 2007; Filosto et al., 2011; Gamou and Shimizu, 1995; Kim et al., 2015; Weng et al., 2018). Diverse modes of EGFR activation have been suggested in which ROS are directly or indirectly involved in EGFR transactivation (Heppner and van der Vliet, 2016; Weng et al., 2018). First, ROS directly modulate a specific cysteine residue (Cys797) within the EGFR kinase domain that is associated with increased tyrosine kinase activity (Paulsen et al., 2011). Next, the ROS induce oxidation of reduction-oxidation targets, such as protein tyrosine (Tyr) phosphatases (PTPs), to enhance EGFR Tyr phosphorylation (Lee et al., 1998). Finally, ROS induce cysteine oxidation within Src and ADAM17, which results in their activation and further EGFR transactivation (Sham et al., 2013).

ROS-involved EGFR transactivation can initiate multiple signaling pathways that are similar to ligand-dependent EGFR tyrosine activation. Ultimately, this signaling helps to protect cells against oxidative stress. Oxidative stress activates AKT via the EGFR/PI3K-dependent pathway in a number of cell types (Wang et al., 2000). After activation of the EGFR/PI3K-dependent pathway, the PI3K/Akt pathway inhibits glycogen synthase kinase 3β (GSK-3β) and thereby induces nuclear translocation of nuclear factor erythroid 2-related factor 2 (Nrf2) (Chowdhry et al., 2013; Ma, 2013). Nuclear factor erythroid 2-related factor 2 subsequently induces the expression of an array of ROS-detoxifying enzymes and stimulates the production of antioxidants, including GSH (Ma, 2013). Activated AKT also phosphorylates and inactivates components of the cell death machinery including Bax, Bad, and caspase 9 (Brunet et al., 1999; Sadidi et al., 2009). Activated AKT also regulates the activity of FOXO3, which is a member of the Forkhead family of transcription factors that induces genes necessary for cell death (Brunet et al., 1999; Hagenbuchner et al., 2012). Therefore, AKT increases the cell's antioxidant capacity and thereby promotes cell survival under oxidative stress in transcription-independent and/or dependent manners. Next, it has been previously shown that H_2O_2-induced EGFR transactivation increases PLC-γ1-mediated pro-survival function. Genetic ablation and pharmacological inhibition of PLC-γ1 enhances a cell's susceptibility to hydrogen peroxide-induced cell death; however, it is not clear how activated PLC-γ1 mitigated the cellular oxidative damage (Goldkorn et al., 1998; Morita et al., 2008; Wang et al., 2001). Oxidative stress also triggers the phosphorylation of STAT proteins (STAT1, STAT3, and STAT5), which can induce genes that control cell growth and survival (Carballo et al., 1999; Miklossy et al., 2013; Rodriguez-Fragoso et al., 2009). During oxidative stress, EGFR transactivation is transferred by Janus kinases 1 and 2 (JAK1/2) or c-Src to STAT-1/3 and STAT-5. JAK1/2 and c-Src kinases modulate STATs activation in at least the following two ways: (1) by direct phosphorylation of STATs and (2) by phosphorylating the EGFR at Y845.

Eukaryotic translation initiation factor 2 alpha (eIF2α) is a subunit of the trimeric eIF2 complex that is involved in the initiation step of cap-dependent mRNA translation (Sonenberg and Hinnebusch, 2009). The eIF2 complex delivers the initiator methionyl-tRNA (Met-tRNAi) to the ribosome during translation initiation of cytoplasmic mRNAs in eukaryotic cells. Mammalian cells respond to various forms of physiological or pathological stress (such as hypoxia, amino acid deprivation, glucose deprivation, viral infection, endoplasmic reticulum [ER] stress, and oxidative stress) by blocking the translational initiation process through phosphorylation of eIF2α at Serine 51. Such stresses are sensed by the four mammalian eIF2α protein kinases: PERK, GCN2, PKR, and HRI, which respond to distinct stimuli (Proud, 2005; Wek et al., 2006). However, it has been reported that oxidative stress also activates multiple eIF2α kinases (including PERK, PKR, and GCN) and regulates the eIF2 complex through eIF2α phosphorylation (Liu et al., 2008; Rajesh et al., 2015). Therefore, several groups, including ours, have reported that genetic loss of the eIF2α kinases or eIF2α phosphorylation make cells susceptible to death by oxidative stress (Choi et al., 2017; Han et al., 2013; Lewerenz and Maher, 2009; Liu et al., 2008; Rajesh et al., 2015). In addition, our group recently suggested that fructose diet-induced hepatocyte death results from a diminished antioxidant capacity in hepatocyte-specific eIF2α phosphorylation deficient mice (Choi et al., 2017). However, we did not identify the upstream signaling pathways whose activation in response to oxidative stress may play important roles in maintaining the antioxidant capacity and alleviating oxidative hepatocyte damage. Here, we report that hepatocyte-specific eIF2α phosphorylation-deficient mice have significantly reduced expression of the EGFR and altered EGFR-mediated signaling pathways. Both the EGFR and EGFR-mediated signaling pathways are required for a cell to appropriately defend against oxidative stress. Therefore, EGFR knockdown cells have decreased ROS scavenging ability and aggravated oxidative stress-mediated cell death. Conversely, enhanced expression of EGFR increased ROS scavenging ability and alleviated ROS-mediated cell death in eIF2α phosphorylation-deficient primary hepatocytes. Therefore, our results suggest that a decreased EGFR level partially explains the susceptibility of eIF2α-phosphorylation-deficient hepatocytes to ROS.

MATERIALS AND METHODS

Animals and *in vivo* EGF treatment

S/A;fTg/0 (*Cont.*) and *A/A;fTg/0;Cre^{Hep}/0* (*A/A^{Hep}*) mice have been previously described (Choi et al., 2017). The animals were housed with 12-h light and 12-h dark cycles, and provided with standard rodent chow (Purina; Cargill Inc., USA) and water ad libitum. All animal care and procedures were conducted according to the protocols and guidelines approved by the University of Ulsan Animal Care and Use Com-

mittee (UOUACUC) (No. SHB-17-010).

The *Cont.* and *A/A*^{Hep} mice fasted for 12 h prior to *in vivo* EGF-mediated EGFR stimulation. After anesthesia was induced, the mice received 0.9% saline or 0.9% saline containing recombinant murine EGF (0.5 μg/g of body weight; PeproTech, Korea) via the vena cava. The liver was removed 5 min after this injection. The specimens were frozen and stored at −80°C until homogenization.

Quantitative real-time polymerase chain reaction

Total RNAs were isolated from liver tissues using the Trizol reagent (Life Technologies, USA). cDNA was prepared with a High Capacity cDNA RT kit (Ambion, USA) for quantitative real-time polymerase chain reaction (qRT-PCR). qRT-PCR was carried out using the SYBR green PCR master mix (Bio-Rad, USA) with the appropriate primers on a StepOnePlus Real Time System (Applied Biosystems, USA). The specificity of each primer pair was confirmed using melting curve analysis. The housekeeping *β-actin* gene was amplified in parallel with the *EGFR* gene. Relative copy numbers, compared to the *β-actin* gene, were calculated using $2^{-\Delta\Delta Ct}$. The primer sequences used were as follows: 5'-AGGACTGGGCAATCTGTTGGA-3' and 5'-GAAGATCGAAGACCTGGTGCTGTAA-3' (*EGFR*); 5'-GATCTGGCACCACACACCTTCT-3' and 5'-GGGGTGTTGAAGGTCTCAAA-3' (*β-actin*).

Western blot analysis and antibodies

Liver tissues and cells were homogenized in Nonidet P40 lysis buffer (1% NP40, 50 mM Tris-Cl pH 7.5, 150 mM NaCl, 0.05% SDS, 0.5 mM Na-vanadate, 100 mM NaF, 50 mM β-glycerophosphate, 1 mM PMSF) that was supplemented with Halt Protease Inhibitor Cocktail (Thermo Fisher Scientific, USA). The homogenates were centrifuged at 12,000*g* for 15 min at 4°C, and the supernatants were collected. The liver lysates or cell lysates were used for Western blotting, as described (Choi et al., 2017). The following were purchased from Sigma-Aldrich (USA): α-Tubulin (T5168), β-Actin (A5441), Flag (F1804). The following were purchased from Santa Cruz Biotechnology (USA): eIF2α (SC-133132), STAT3 (SC-482), STAT5 (SC-835). The following were purchased from Cell Signaling Technology (USA): Phospho-EGFR (Y1068) (#3777), AKT (#4691), Phospho-AKT (S473) (#4060), ERK (#4695), Phospho-ERK (T202/Y204) (#4407), Phospho-STAT3 (Y705) (#4113), Phospho-STAT5 (Y694) (#9314). The following were purchased from Merck Milipore (USA): EGFR (06-847). The following were purchased from Abcam (UK): p-eIF2α (S31) (ab32157). The secondary peroxidase-conjugated antibodies were purchased from Thermo Fisher Scientific or Jackson ImmunoResearch (USA).

Chemicals

Dichlorodihydrofluorescein diacetate (DCF-DA) was purchased from Thermo Fisher Scientific. The following were purchased from Sigma-Aldrich: crystal violet, parformaldehyde, polybrene (hexadimethrine bromide), hydrogen peroxide, menadione, propidium iodide (PI), Hoechst 33258, 4′,6-diamidino-2-phenylindole (DAPI), dihydroethidine hydrochloride (DHE), and N-acetyl-L-cysteine (NAC).

Preparation of primary hepatocytes

The primary mouse hepatocytes were obtained as has been described previously (Choi et al., 2017). The isolated primary hepatocytes were inoculated on collagen-coated plates with/without round coverslips (5×10^5 cells/well in 6-well plates), and cultured in high glucose-DMEM (WelGENE, Korea) medium containing 10% FBS (WelGENE), and 1% penicillin/streptomycin (WelGENE). The medium was replaced with FBS-free DMEM media 2 h after plating. The hepatocytes were incubated for another 12 h before the experimental treatment.

Cell lines and cell culture

Immortalized embryonic hepatocytes were cultured in Medium 199 (WelGENE) that was supplemented with 10% fetal bovine serum (WelGENE) and 1% penicillin-streptomycin (WelGENE), as previously described (Back et al., 2009). AML12 muse normal hepatocytes were obtained from the American Type Culture Collection (ATCC, USA). The cells were cultured in DMEM/F12 (WelGENE) that was supplemented with 10% fetal bovine serum (WelGENE), 100 nM dexamethason (Sigma-Aldrich), 1% insulin-transferrin-selenium-pyruvate supplement (ITSP; WelGENE), and 1% penicillin-streptomycin (WelGENE). The Lenti-X 293T Cell Line (Clontech, USA) was cultured in DMEM (WelGENE) containing 10% fetal bovine serum (WelGENE) and 1% penicillin-streptomycin (WelGENE).

Generation of *EGFR* knockdown cell lines

The five MISSION shRNA clones of mouse EGFR (NM_007912.1; a protein of 1210 amino acids) that were inserted into the pLKO.1 vector (TRCN0000023479 to TRCN0000023483) were purchased from Sigma-Aldrich. A negative control (NC) shRNA sequence that was cloned into the pLKO.1 vector was included as a control. Each pLKO.1 shRNA construct was cotransfected with the Lenti-X Packaging Single Shots (VSV-G) (Clontech) into the Lenti-X 293T cells. The lentiviral particles were produced according to the manufacturer's instructions. The immortalized embryonic hepatocytes and AML12 cells were infected with recombinant lentiviruses in the presence of polybrene (8.0 μg/ml) for 2 days. Next, the hepatocytes were cultured with fresh complete media containing puromycin (1.0 μg/ml for hepatocyte and 0.75 μg/ml for AML12) for 3 to 4 weeks to select for *EGFR* knockdown cells. The EGFR expression level was routinely tested using Western blot. We chose immortalized embryonic hepatocytes that stably expressed the *EGFR* shRNA targeting the sequence GCTTTCGAGAACCTAGAAATA (TRCN0000023483, referred to as shEGFR-83), or AML12 cells that stably expressed the *EGFR* shRNA targeting the sequence CCTGTCCAACTATGGGACAAA (TRCN0000023481, referred to as shEGFR-81) for further experiments.

Production of recombinant adenovirus expressing mouse EGFR-Flag

The C-terminal Flag tagged mouse EGFR (mEGFR-Flag) expression vector pCMV3-mEGFR-Flag was purchased from Sino Biological. The pShuttle-CMV-mEGFR-Flag vector was then constructed by inserting the cDNA fragment encoding mEGFR-Flag from the pCMV3-mEGFR-Flag treated with *Bgl*

II-Fill in-Not I into the pShuttle-CMV treated with *Hind III-Fill in-Not I*. The AdEasy vector system was used to generate the mEGFR-Flag expressing recombinant adenovirus according to the manufacturer's instructions (Agilent Technologies, USA). In brief, the shuttle vector was then electrophoresed into BJ5183 cells that contained the adenoviral vector Adeasy to generate a recombinant adenoviral plasmid. The recombinants were amplified in HEK-293A cells and purified by CsCl (Sigma-Aldrich) gradient centrifugation. Viral preparations were collected and desalted, and titers were determined using the AdEasy Viral Titer Kit (Agilent Technologies) according to the manufacturer's instructions. The efficiency of adenoviral infection was assessed by immunofluorescence detection of the C-terminal Flag tag of mEGFR.

Cell viability and death analysis

Cell viability analysis using crystal violet was performed as has been previously described with slight modifications (Oh et al., 2006). In brief, the drug-treated cells were washed twice with cold phosphate-buffered saline (PBS). The cells were stained with crystal violet solution (0.625 g of crystal violet dissolved in a solution containing 50 ml of 37% paraformaldehyde and 450 ml of methanol) for 4 min at room temperature. The stained cells were washed three times in tap water, and the plates were allowed to dry. Microscopic images of the stained cells were taken with a Primovert inverted microscope (Zeiss, Germany) equipped with an Axiocam ERc 5s camera. The cells were then lysed with 1% SDS solution, and dye uptake was measured at 550 nm using a microplate reader (SpectraMax iD3; Molecular Devices, USA).

Cell death analysis using PI and Hoechst 33258 were performed as previously described (Choi et al., 2017). The drug-treated cells on the coverslips were double-stained with PI (1 μg/ml) and Hoechst 33258 (1 μg/ml), and fixed with 3.5% (w/v) paraformaldehyde at room temperature for 15 min. The coverslips were then mounted on glass slides for observation under fluorescence microscopy (Olympus microscope; Olympus, Japan). At least 500 cells were counted. A quantitation of dead cells (apoptotic and necrotic cells) was expressed as a percentage of total cells counted.

Microscopy and image analysis

Intracellular ROS levels were measured using confocal microscopy using the fluorescent probes DHE or DCF-DA, as described previously (Choi et al., 2017). The drug-treated primary hepatocytes and immortalized hepatocytes were plated on collagen coated 35 mm coverglass bottom dishes (SPL, Korea) and cultured overnight. The next day, the cells were treated with the indicated chemicals. After treatment, the cells were stained with DHE (15 μM) or DCF-DA (15 μM) in phenol red-free culture medium for 30 min. Fluorescence images of the living cells were obtained using an FV1200-OSR confocal laser microscope (Olympus).

For the immunofluorescence detection of mEGFR-Flag proteins, immortalized embryonic hepatocytes (2×10^5) were plated on 6-well plates coated with 0.01% collagen in PBS and cultured overnight. The next day, the cells were infected with adenovirus encoding mEGFR-Flag (Ad-mEGFR-Flag) at a multiplicity of infection of 100 for 12 h. The cells were then fixed with 4% paraformaldehyde in PBS for 15 min, and permeabilized with 0.1% Triton X-100 in PBS for 4 min. The cells were blocked with 3% bovine serum albumin in PBS for 30 min, and incubated with the indicated primary antibody overnight at 4°C. The cells were further incubated with a Tetramethylrhodamine (TRITC)-conjugated secondary antibodies at room temperature for 1 h. The nuclei were stained with DAPI (Sigma-Aldrich). Finally, the cells were observed by confocal laser microscopy using an FV1200-OSR microscope.

The scale bars (μm) have been inserted into the microscopic images.

Statistical analysis

Experiments were repeated three times in each case. The data were analyzed using GraphPad Prism 5 (GraphPad Software, USA). Unpaired 2-tailed Student's *t*-tests were performed to determine the statistical significance of the paired samples. $P < 0.05$ was considered statistically significant. Error bars represent the SEM in every case.

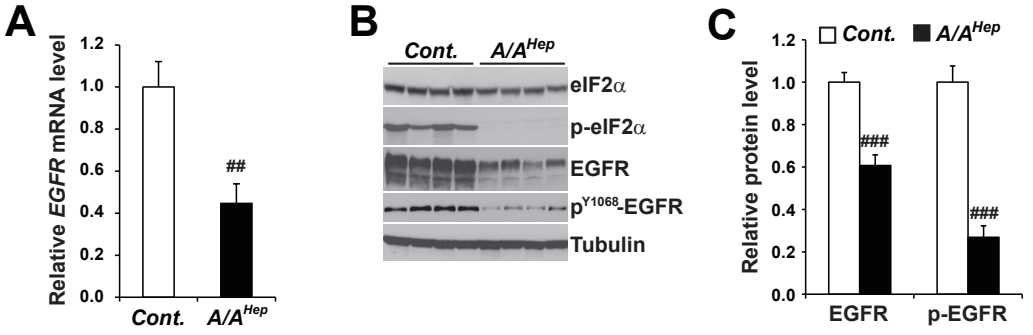

Fig. 1. Expression levels of EGFR mRNA and protein are reduced in liver tissues of hepatocyte-specific eIF2α phosphorylation-deficient mice. (A) Quantitative real-time PCR analysis of the expression of *Egfr* mRNAs in liver tissues from 3-month-old *Cont.* and *A/A^{Hep}* mice. Data are expressed as mean ± SEM (n = 6 mice per group). $^{\#\#}P < 0.01$; *Cont.* vs *A/A^{Hep}*. (B) Western blot analysis of eIF2α, p-eIF2α, EGFR, p-EGFR, and tubulin in liver tissues from 3-month-old *Cont.* and *A/A^{Hep}* mice. The efficiency of deletion of *floxed eIF2α fTg* by Cre recombinase in *A/A^{Hep}* livers was determined based on the existence of phosphorylated eIF2α proteins (Choi et al., 2017). (C) Densitometric quantification of EGFR and p-EGFR protein expression levels in Fig. 1B. Values were normalized against tubulin levels. Data are expressed as mean ± SEM (n = 4 mice per group). $^{\#\#\#}P < 0.001$; *Cont.* vs *A/A^{Hep}*.

RESULTS AND DISCUSSION

The hepatocyte-specific eIF2α phosphorylation-deficient mouse model has reduced EGFR expression and altered EGF/EGFR-mediated signaling pathways

The mRNA levels of EGFR (or the ErbB1 receptor) were diminished to ~40% in the liver tissues of hepatocyte-specific eIF2α phosphorylation (p-eIF2α)-deficient mice (Fig. 1A). Similarly, the levels of the EGFR (~60%) and phosphorylated EGFR (P^{Y1068}-EGFR, ~30%) proteins were significantly reduced in p-eIF2α deficient liver tissues (Figs. 1B and 1C).

In order to examine the effect of decreased EGFR in intact livers, starved control and *A/A*^{Hep} mice were injected with either saline or recombinant EGF. Five minutes after this injection, the livers were harvested from the saline- and EGF-treated animals. We analyzed the EGF/EGFR signaling pathways using Western blots with total liver tissue lysates. In agreement with previous studies done in cell culture (Guren et al., 2003; Kitade et al., 2013; Musallam et al., 2001) and animal livers (Fan et al., 2013; Ostrowski et al., 2000; Quesnelle et al., 2007), starvation abolished phosphorylation of the following targets in the liver tissues of all saline-treated animals: EGFR at Tyr1068; the EGF/EGFR-downstream targets AKT at Ser473; STAT3 at Tyr705; STAT5 at Tyr694; and ERK at Thr202/Tyr204 (Fig. 2). However, the EGF treatments rapidly induced EGFR phosphorylation in the livers of both starved *control* and *A/A*^{Hep} mice. However, the EGFR phosphorylation levels of *A/A*^{Hep} livers were significantly lower than were those in the control livers. This difference is explained by a reduced level of EGFR protein in *A/A*^{Hep} livers compared to that in the control livers (Fig. 2A, left graph). With the exception of ERK phosphorylation (Fig. 2E), the phosphorylation levels of AKT, STAT3, and STAT5 were also significantly lower in *A/A*^{Hep} livers than they were in control livers (Figs. 2B-2D). These data suggest that eIF2α phosphorylation may be required to keep the EGFR expression level normal, and to maintain the activity of the EGF-dependent EGFR signaling pathways in hepatocytes.

eIF2α phosphorylation-deficient primary hepatocytes are susceptible to oxidative stress

Several groups have reported that EGFR can be activated by oxidative stress (Abdelmohsen et al., 2003; Chiarugi and

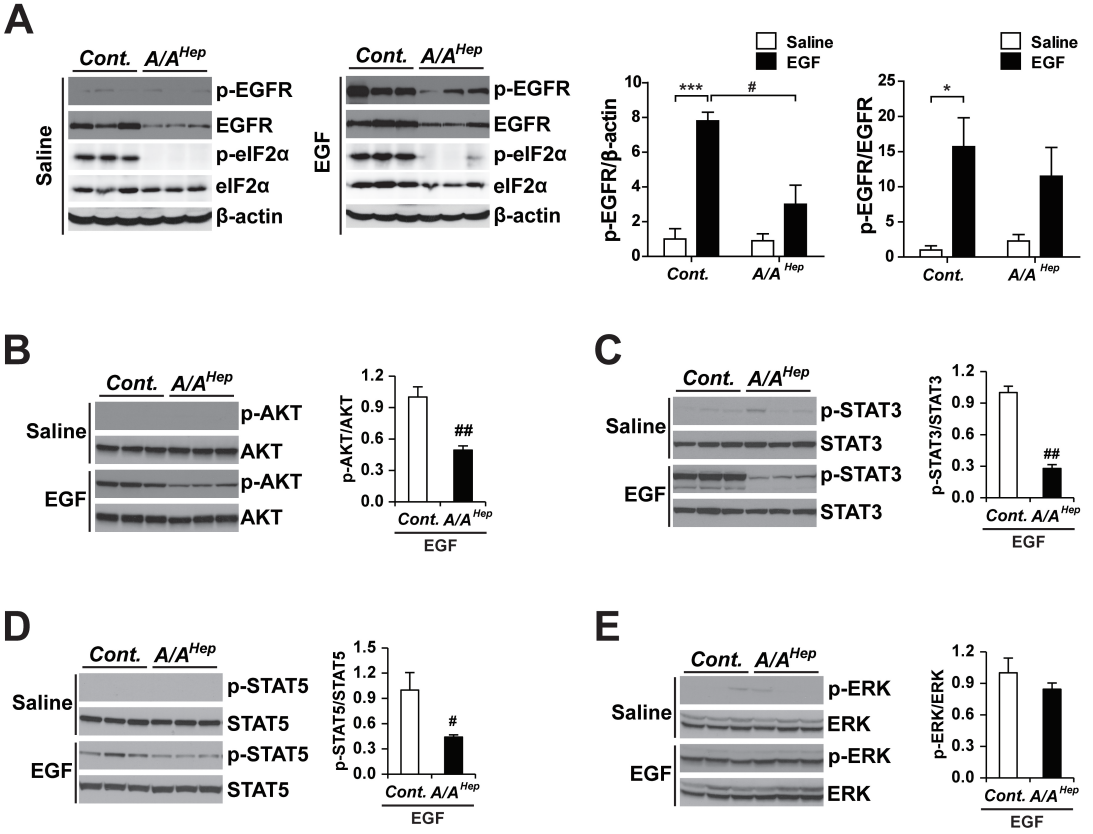

Fig. 2. EGFR signaling pathways are altered in liver tissues of hepatocyte-specific eIF2α phosphorylation-deficient mice. For EGFR signaling pathway analysis, fasted and anesthetized *Cont.* and *A/A*^{Hep} mice were administered saline or recombinant murine EGF (0.5 μg/g) via the vena cava. The livers were removed 5 min after this injection. The liver lysates were subjected to SDS-PAGE, followed by immunoblot analyses using antibodies specific for p-EGFR, EGFR, p-eIF2α, eIF2α, and β-actin (A), p-AKT and AKT (B), p-STAT3 and STAT3 (C), p-STAT5 and STAT5 (D), and p-ERK and ERK (E). The ratios of p-EGFR/β-actin and p-EGFR/EGFR (A), p-AKT/AKT (B), p-STAT3/STAT3 (C), p-STAT5/STAT5 (D), and p-ERK/ERK (E) were densitometrically quantified. Data are expressed as mean ± SEM (n = 3 mice per group). $*P < 0.05$ and $***P < 0.001$; Saline vs EGF and $^{\#}P < 0.05$ and $^{\#\#}P < 0.01$; *Cont.* vs *A/A*^{Hep}.

Buricchi, 2007; Filosto et al., 2011; Gamou and Shimizu, 1995; Kim et al., 2015; Wang et al., 2000; Weng et al., 2018) (Supplementary Fig. S1). In contrast, the inhibition or genetic disruption of EGFR is involved in the induction of oxidative stress and cytotoxicity *in vitro* and *in vivo* (Orcutt et al., 2011; Schreier et al., 2013). Previous work from our group suggests that eIF2α phosphorylation protects hepatocytes from oxidative stress (Choi et al., 2017). Therefore, we measured the ROS-scavenging activity and oxidative stress-mediated cell death in p-eIF2α-deficient primary hepatocytes. We compared these features to those of control hepatocytes. There was no significant difference between the *Cont.* and *A/A*^{Hep} hepatocytes (under mock conditions) with regard to the microscopic evaluation of dihydroethidium (DHE) fluorescence in the detection of superoxides (Fig. 3A). However, when accumulated ROS levels were compared in menadione (Men) or hydrogen peroxide (H_2O_2)-treated conditions, the DHE fluorescence intensities were significantly higher in the *A/A*^{Hep} hepatocytes than they were in the *Cont.* although treatment with antioxidant N-acetylcysteine (NAC) removed the difference (Fig. 3A), suggesting that p-eIF2α-deficient primary hepatocytes have reduced ROS-scavenging activity than do control hepatocytes. We next investigated the influence of eIF2α phosphorylation on menadione or H_2O_2-induced cell death. Menadione or H_2O_2 treatment reduced the number of crystal violet stained cells in a dose-dependent manner (Fig. 3B). However, menadione or H_2O_2 treatment caused larger reductions in the cell viability of eIF2α phosphorylation-deficient *A/A*^{Hep} hepatocytes than it did in control cells (Fig. 3B). Cell death analysis was performed using the Hoechst 33258/PI staining procedure. The *A/A*^{Hep} hepatocytes also demonstrated more cell death than did the control hepatocytes in menadione or H_2O_2 treated conditions (Fig. 3C). Therefore, eIF2α phosphorylation-deficient primary hepatocytes were more susceptible to oxidative stress (than were control cells) because of reduced ROS-scavenging activity.

EGFR knockdown reduces ROS-scavenging activity and increases vulnerability to oxidative stress

We previously showed that vulnerability to oxidative stress in *A/A*^{Hep} primary hepatocytes is related to decreasing EGFR protein levels. Therefore, we knocked down the EGFR gene in both immortalized mouse embryonic hepatocyte cell lines (Back et al., 2009; Choi et al., 2017) (Fig. 4), and in the mouse hepatocyte cell line AML12 (Supplementary Fig. S2). We then assessed these cells with regard to their ROS-scavenging activity and ROS-mediated cell death. First, we observed the concentrations and time-dependent changes of EGFR and eIF2α phosphorylation in both cell lines (Supplementary Fig. S1). With regard to menadione and H_2O_2 treatments in immortalized hepatocytes, the activation of eIF2α phosphorylation was rapid and persistent in all tested conditions (of different concentrations and times) (Supplementary Figs. S1A and S1C). However, the induction of eIF2α phosphorylation in the drug-treated AML12 cells was observed after 2 h of treatment, but not at any other time points (Supplementary Figs. S1B and S1D). The EGFR phosphorylation gradually increased in a concentration- and time-dependent manner during drug treatment (Supplementary Figs. S1A-S1C), except for the time-dependent treatments in AML12 cells (Supplementary Fig. S1D). Similar to eIF2α phosphorylation, the EGFR phosphorylation was the highest after 2 h of treatment. After this, the EGFR phosphorylation progressively decreased at increased treatment times in AML12 cells (Supplementary Fig. S1D). Therefore, these results indicate that oxidative stressors induce EGFR and eIF2α phosphorylation in a similar concentration- and time-dependent manner. However, there is no evidence that eIF2α phosphorylation regulates that of EGFR yet.

Next, in order to examine whether the level of EGFR expression can affect a cell's antioxidant capacity, we established EGFR knockdown cell lines. These knockdown cell lines were created by transducing EGFR targeting shRNA-expressing lentiviruses and following puromycin selection in both immortalized mouse embryonic hepatocytes (Fig. 4A) and AML12 cells (Supplementary Fig. S2A). Among the established EGFR knockdown cell lines, the cell lines with the lowest expression of EGFR protein were chosen for further experiments. These included the shEGFR-83 cell line for immortalized hepatocytes (Fig. 4A) and the shEGFR-81 cell line for AML12 cells (Supplementary Fig. S2A). In order to assess the ROS-scavenging activity of the EGFR knockdown cell lines, the levels of accumulated ROS were compared to the fluorescence intensity of an oxidant-sensing probe DCF-DA in H_2O_2-treated shNC control or shEGFR-83 cell lines. Under H_2O_2-treated conditions, the fluorescence intensity of shEGFR-83 cells was significantly higher than that of shNC control cells (Fig. 4B). However, there was no significant difference in the fluorescence intensity between them before H_2O_2 treatment or after H_2O_2 and N-acetyl-L-cysteine (NAC) co-treatment. In addition, the fluorescent microscopic examination of menadione-treated cells (using a superoxide indicator DHE) revealed that DHE fluorescence in the EGFR knockdown cells (shEGFR) was stronger than that in shNC control cells (Fig. 4C). These results indicate that EGFR protein levels are important to maintain a cell's hydrogen peroxide- or superoxide-scavenging activity.

Having observed that EGFR knockdown cells have reduced ROS-scavenging activity, we next examined whether knockdown of EGFR increases a cell's vulnerability to oxidative stress. To do so, we applied the crystal violet assay and Hoechst 33258/PI staining analysis to compare cell death between EGFR knockdown cells and controls (Figs. 4D and 4E, Supplementary Figs. S2A, S2B, and S3). As expected, the crystal violet assay showed that the shEGFR-83 cells had poorer cell viability than did shNC control cells under menadione or H_2O_2 treatment although the cell viability of shNC control cells was also reduced in a dose-dependent manner in these treatments. However, the levels in the shEGFR-83 cells were similar to those in shNC control cells in NAC-treated conditions. The cell death analysis (using the Hoechst 33258/PI staining procedure) also revealed that shEGFR-83 cells had a higher rate of cell death than did the shNC control cells in menadione or H_2O_2 treated conditions (Fig. 4E). However, the levels in the shEGFR-83 cells were similar to those in shNC control cells in NAC-treated conditions. We obtained similar results in the shEGFR-81 cell line of AML12 cells (Supplementary Figs. S3B and S3C). The shEGFR-81 cells

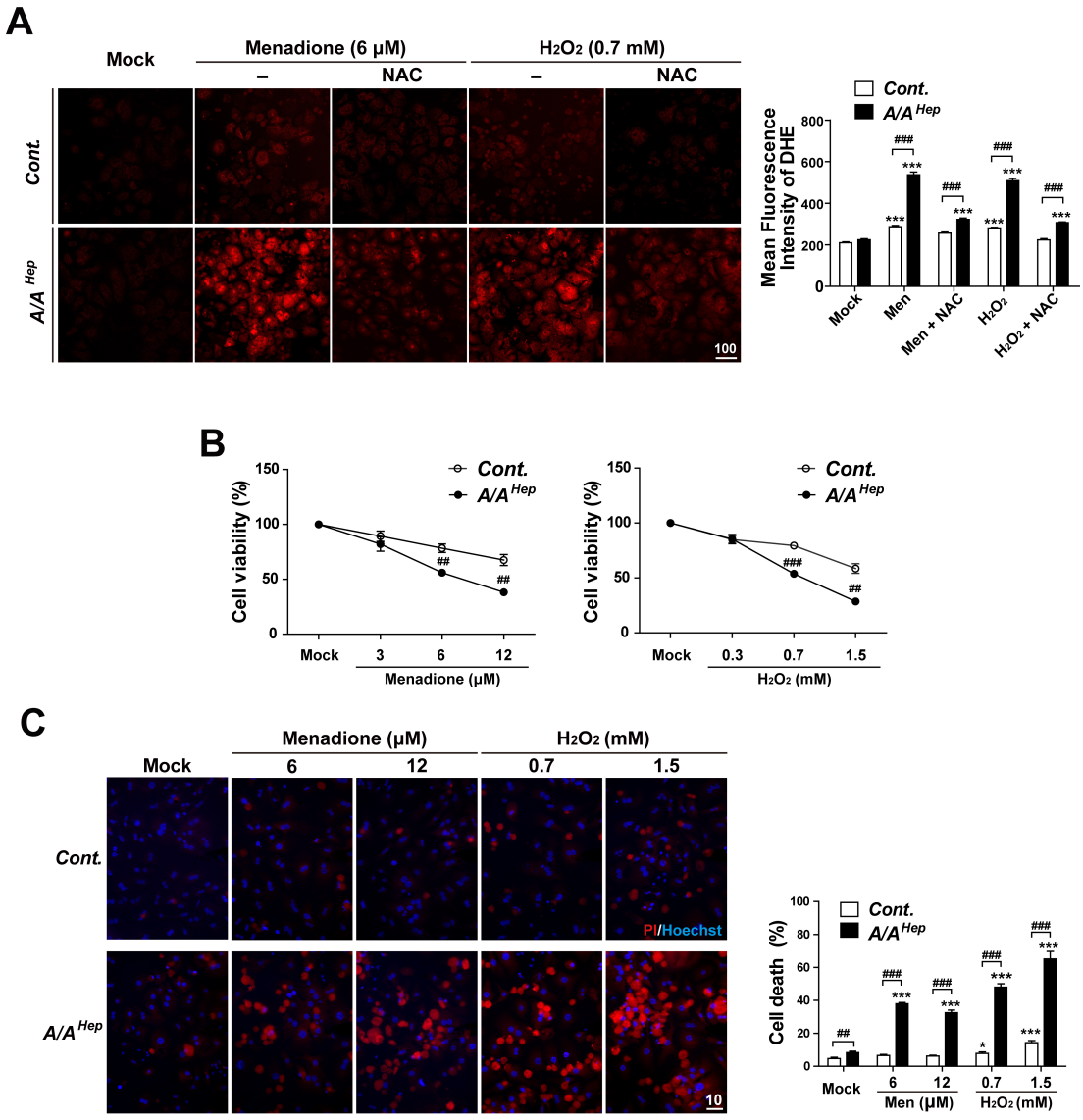

Fig. 3. eIF2α phosphorylation-deficient primary hepatocyte has reduced ROS-scavenging activity, which may increase vulnerability to oxidative stress. (A) Primary hepatocytes isolated from *Cont.* and *A/A*^{Hep} mice were treated with menadione (6 μM), menadione (6 μM) plus N-acetylcysteine (NAC, 1 mM), hydrogen peroxide (H_2O_2, 0.7 mM), or hydrogen peroxide (H_2O_2, 0.7 mM) plus N-acetylcysteine (NAC, 1 mM) for 16 h. Accumulated intracellular ROS were observed by fluorescence microscopy of cells stained with dihydroethidium (DHE), reflecting ROS levels. The representative images are shown (scale bar = 100 μm). For graphs, the mean fluorescence intensities (MFI) of DHE staining were measured using image analysis software. The data are expressed as mean ± SEM of three independent experiments. $^{***}P < 0.001$; Mock vs Chemicals in the same genotype, $^{###}P < 0.001$; *Cont.* vs *A/A*^{Hep}. (B) Primary hepatocytes isolated from *Cont.* and *A/A*^{Hep} mice were treated with menadione or hydrogen peroxide (H_2O_2) at indicated concentrations for 30 h. The cell viability was determined using the crystal violet assay. The data are expressed as mean ± SEM of three independent experiments. $^{##}P < 0.01$ and $^{###}P < 0.001$; *Cont.* vs *A/A*^{Hep}. (C) The primary hepatocytes isolated from *Cont.* and *A/A*^{Hep} mice were treated with menadione or hydrogen peroxide (H_2O_2) at indicated concentrations for 24 h. Cell death (apoptotic and necrotic cells) was determined by double staining with Hoechst 33258 and propidium iodide (PI). Representative images are shown (scale bar = 10 μm). At least 500 cells were counted. Cell death is expressed as a percentage of total cells. The data are expressed as mean ± SEM of three independent experiments. $^{*}P < 0.05$ and $^{***}P < 0.001$; Mock vs Chemicals in the same genotype, $^{##}P < 0.01$ and $^{###}P < 0.001$; *Cont.* vs *A/A*^{Hep}.

were more susceptible to menadione- or H_2O_2-mediated oxidative stress than were shNC control cells. These cell death analyses suggested that the EGFR protein is important to alleviate oxidative stress-mediated cell death. Collectively, our experiments suggest that attenuated EGFR expression reduces cellular ROS-scavenging activity, which then increases cells' vulnerability to oxidative stress.

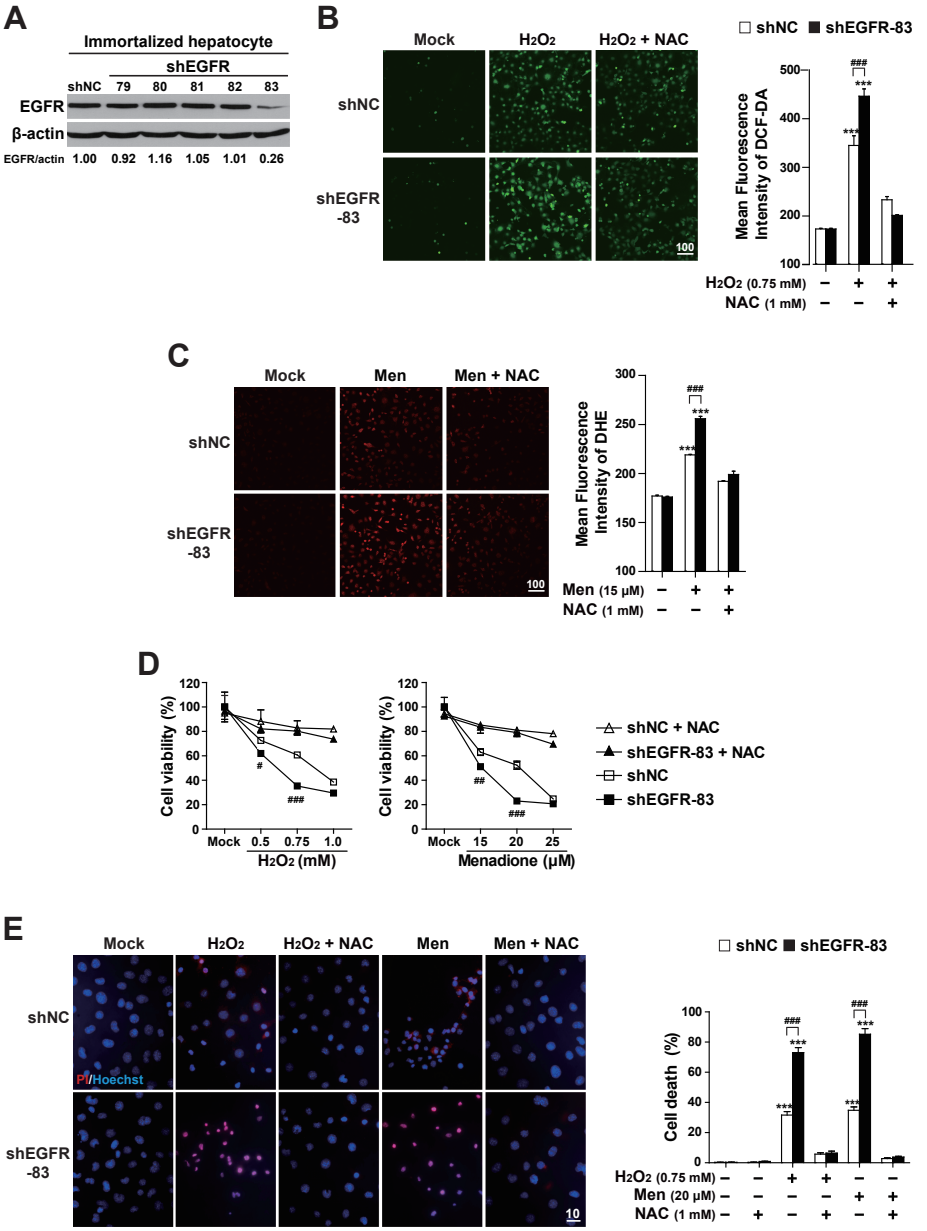

Fig. 4. EGFR depletion enhances susceptibility to reactive oxygen species. (A) From immortalized embryonic hepatocytes stably expressing five EGFR shRNAs (79-83) or shNC, the cell lysates were subjected to SDS-PAGE, followed by immunoblot analyses using antibodies specific for EGFR and β-actin. For the EGFR/β-actin ratio, densitometry scanning was performed and quantified with NIH Image software. (B) The shNC and shEGFR-83 cell lines were treated with hydrogen peroxide (H_2O_2, 0.75 mM) or hydrogen peroxide (H_2O_2, 0.7 mM) plus N-acetylcysteine (NAC, 1 mM) for 4 h. (C) The shNC and shEGFR-83 cell lines were treated with menadione (6 μM), or menadione (15 μM) plus N-acetylcysteine (NAC, 1 mM) for 3 h. The accumulated intracellular ROS was observed by fluorescence microscopy of cells stained with DCF-DA (B) and dihydroethidium (DHE) (C), reflecting ROS levels. Representative images are shown (scale bar = 100 μm). The mean fluorescence intensities (MFI) of DCF-DA or DHE staining were measured using image analysis software. The data are expressed as mean ± SEM of three independent experiments. $^{***}P < 0.001$; Mock vs Chemicals in the same genotype, $^{###}P < 0.001$; shNC vs shEGFR. (D) The shNC and shEGFR-83 cell lines were treated with hydrogen peroxide (H_2O_2) or menadione at indicated concentrations with/without NAC (1 mM) for 7 h. Cell viability was determined using the crystal violet assay. The data are expressed as mean ± SEM of three independent experiments. $^{#}P < 0.05$, $^{##}P < 0.01$, and $^{###}P < 0.001$; shNC vs shEGFR. (E) The shNC and shEGFR-83 cell lines were treated with hydrogen peroxide (H_2O_2, 0.75 mM), menadione (15 μM), H_2O_2 (0.75 mM) plus NAC (1 mM) or menadione (15 μM) plus NAC (1 mM) for 7 h. Cell death (apoptotic and necrotic cells) was determined by double staining with Hoechst 33258 and propidium iodide (PI). Representative images are shown (scale bar = 10 μm). At least 500 cells were counted, and cell death is expressed as a percentage of total cells. The data are expressed as the mean ± SEM of three independent experiments. $^{***}P < 0.001$; Mock vs Chemicals in the same genotype, $^{###}P < 0.001$; shNC vs shEGFR.

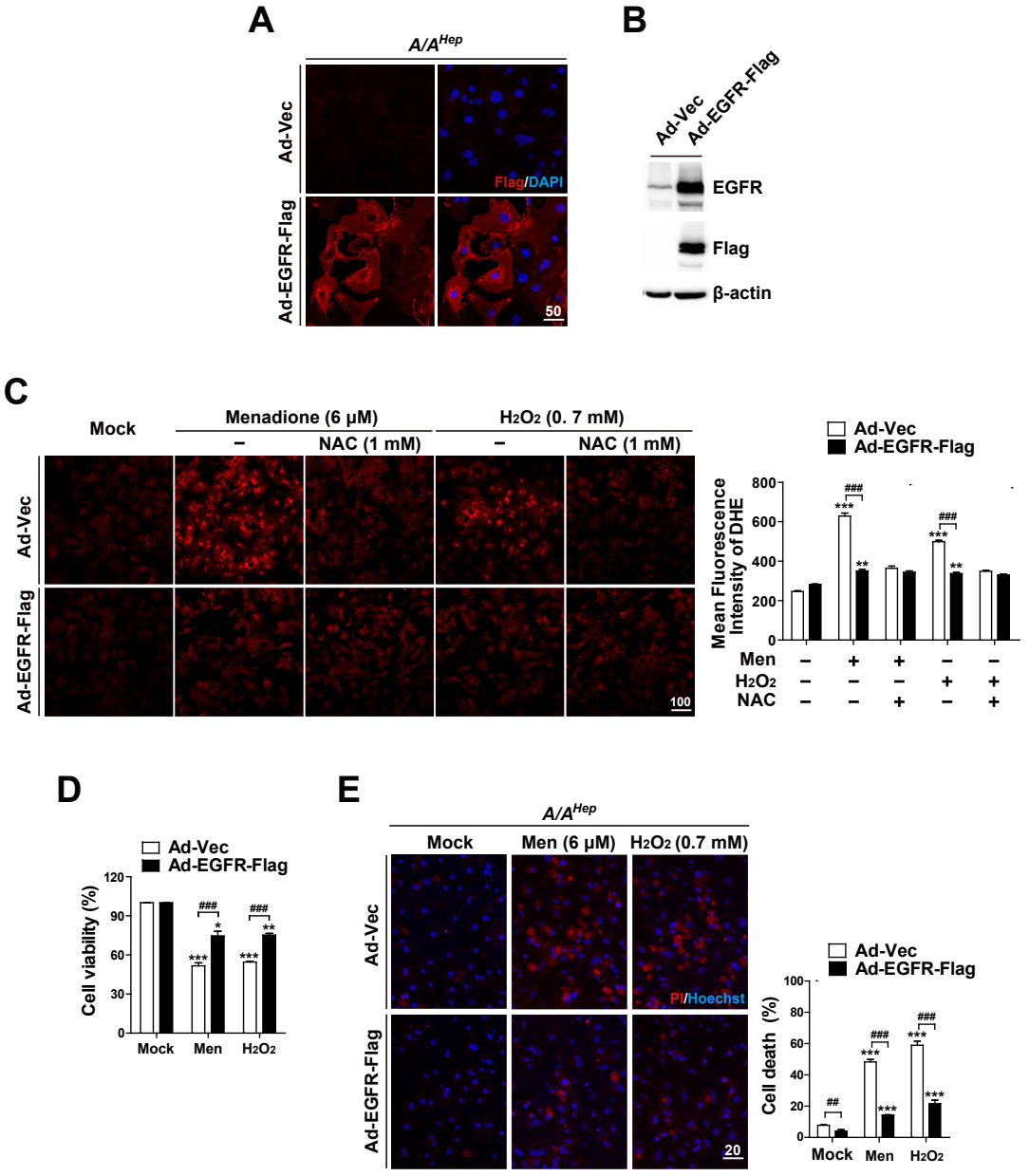

Fig. 5. EGFR overexpression reduces the susceptibility of eIF2α phosphorylation-deficient primary hepatocytes to reactive oxygen species. (A) Primary hepatocytes isolated from *A/A*^{Hep} mice were infected with recombinant adenoviruses (100 multiplicity of infection) expressing EGFR-Flag (Ad-EGFR-Flag) or empty vector controls (Ad-Vec) for 12 h. The cells were fixed, stained with anti-Flag monoclonal antibody and DAPI, and examined by fluorescence microscopy (scale bar = 50 μm). (B) From Ad-EGFR-Flag or Ad-Vec infected *A/A*^{Hep} primary hepatocytes, the cell lysates were subjected to SDS-PAGE, followed by immunoblot analyses using antibodies specific for EGFR, Flag, and β-actin. (C) The Ad-EGFR-Flag or Ad-Vec infected *A/A*^{Hep} primary hepatocytes were treated with menadione (6 μM), menadione (6 μM) plus N-acetylcysteine (NAC, 1 mM), hydrogen peroxide (H_2O_2, 0.7 mM), or hydrogen peroxide (H_2O_2, 0.7 mM) plus N-acetylcysteine (NAC, 1 mM) for 20 h. The accumulated intracellular ROS were observed using fluorescence microscopy of the cells stained with dihydroethidium (DHE), reflecting ROS levels. Representative images are shown (scale bar = 100 μm). The mean fluorescence intensities (MFI) of DHE staining were measured using image analysis software. The data are expressed as the means ± SEMs of three independent experiments. $^{**}P < 0.01$ and $^{***}P < 0.001$; Mock vs Chemicals in the same genotype, $^{\#\#\#}P < 0.001$; Ad-Vec vs Ad-EGFR-Flag. (D and E) The Ad-EGFR-Flag or Ad-Vec infected *A/A*^{Hep} primary hepatocytes were treated with menadione (6 μM) or hydrogen peroxide (H_2O_2, 0.7 mM) for 30 h (D) and 18 h (E). Cell viability was determined using the crystal violet assay. The data are expressed as mean ± SEM of three independent experiments. Cell death (apoptotic and necrotic cells) was determined by double staining with Hoechst 33258 and propidium iodide (PI). Representative images are shown (scale bar = 20 μm). At least 500 cells were counted, and cell death is expressed as a percentage of total cells. The data are expressed as mean ± SEM of three independent experiments. $^{*}P < 0.05$, $^{**}P < 0.01$, and $^{***}P < 0.001$; Mock vs Chemicals in the same group, $^{\#\#}P < 0.01$ and $^{\#\#\#}P < 0.001$; Ad-Vec vs Ad-EGFR-Flag.

EGFR overexpression increases ROS-scavenging activity and alleviates ROS-mediated cell death in eIF2α phosphorylation-deficient primary hepatocyte

We next investigated whether transient enforced expression of EGFR in p-eIF2α deficient primary hepatocytes can increase cellular ROS-scavenging activity and therefore reduce their sensitivity to oxidative stress. Primary hepatocytes purified from livers of hepatocyte specific p-eIF2α deficient (*A/A^{Hep}*) mice were infected with C-terminal Flag-tagged EGFR expressing recombinant adenovirus (Ad-EGFR-Flag) or control adenovirus (Ad-Vec). As expected, immunofluorescence analysis against anti-Flag antibody demonstrated that EGFR-Flag proteins were expressed in almost all *A/A^{Hep}* primary hepatocytes infected by Ad-EGFR-Flag, but not in those infected by Ad-Vec (Fig. 5A). Therefore, Western blot analysis showed that the total amount of EGFR proteins was strongly higher in the Ad-EGFR-Flag infected cell lysates than it was in the Ad-Vec infected cell lysates (Fig. 5B). We next examined whether the enforced expression of EGFR can upregulate cellular ROS-scavenging activity in p-eIF2α deficient (*A/A^{Hep}*) primary hepatocytes. Microscopic observation of DHE fluorescence revealed that there was no significant difference in the fluorescence intensity between Ad-Vec infected hepatocytes and Ad-EGFR-Flag infected hepatocytes under mock conditions (Fig. 5C). However, when the accumulated ROS levels were compared in menadione (Men) or hydrogen peroxide (H_2O_2)-treated conditions, the DHE fluorescence intensities were significantly lower in the Ad-EGFR-Flag infected hepatocytes than in the Ad-Vec infected hepatocytes. The levels in the Ad-EGFR-Flag infected hepatocytes were similar to those in NAC-treated hepatocytes (Fig. 5C). These findings suggest that the enforced expression of EGFR potentiates cellular ROS-scavenging activity of p-eIF2α deficient (*A/A^{Hep}*) primary hepatocytes. In line with these results, the enforced expression of EGFR increased cell viability in menadione (Men) or hydrogen peroxide (H_2O_2)-treated *A/A^{Hep}* primary hepatocytes (Fig. 5D, Supplementary Fig. S4). Moreover, the EGFR-Flag expressing *A/A^{Hep}* primary hepatocytes demonstrated less cell death than did the *A/A^{Hep}* primary hepatocytes under oxidative stress conditions (Fig. 5E). Based on these observations, we conclude that EGFR proteins are required to maintain ROS-scavenging activity in hepatocytes. These proteins are also important to attenuate oxidative stress-mediated cell death.

In this study, we showed that hepatocyte-specific eIF2α phosphorylation-deficient mice have significantly reduced expression of the EGFR and altered EGFR-mediated signaling pathways. Moreover, the eIF2α phosphorylation-deficiency or reduced expression of the EGFR decreased ROS-scavenging activity and increased ROS-mediated cell death in hepatocytes. However, the drawbacks were alleviated by enforced expression of EGFR in p-eIF2α deficient primary hepatocytes. Therefore, we concluded that reduced EGFR level in eIF2α phosphorylation-deficient hepatocytes is one of the critical factors responsible for a cell's susceptibility to oxidative stress. Furthermore, vulnerability to oxidative stress in hepatocytes that have reduced EGFR level or EGFR activity might be the underlying mechanism of hepatotoxicity induced by several EGFR inhibitors (e.g., erlotinib, lapatinib, and gefitinib) used for the treatment of non-small cell lung cancer and pancreatic cancer (Kim et al., 2018; Paech et al., 2017), since most EGFR inhibitors undergo intense metabolism by cytochrome P450 enzymes in hepatocytes (Li et al., 2007; Rakhit et al., 2008) which produces reactive metabolites (Haouzi et al., 2000). However, further studies are required to verify whether the hepatotoxicity is related to oxidative stress susceptibility in EGFR inhibitor-treated hepatocytes.

Note: Supplementary information is available on the Molecules and Cells website (www.molcells.org).

Disclosure

The authors have no potential conflicts of interest to disclose.

ACKNOWLEDGMENTS

This work was supported by the Basic Science Research Program (2014R1A1A4A01004329 and 2017R1D1A1B03028229), the Bio & Medical Technology Development Program (2017M3A9G7072745), and the Priority Research Centers Program (2014R1A6A1030318) of the National Research Foundation of Korea (NRF) funded by the Korean government.

ORCID

Mi-Jeong Kim https://orcid.org/0000-0003-1610-7649
Woo-Gyun Choi https://orcid.org/0000-0003-4689-6394
Kyung-Ju Ahn https://orcid.org/0000-0002-3561-0963
In Gyeong Chae https://orcid.org/0000-0002-4496-4448
Rina Yu https://orcid.org/0000-0002-1965-3891
Sung Hoon Back https://orcid.org/0000-0001-8029-1298

REFERENCES

Abdelmohsen, K., Gerber, P.A., von Montfort, C., Sies, H., and Klotz, L.O. (2003). Epidermal growth factor receptor is a common mediator of quinone-induced signaling leading to phosphorylation of connexin-43: role of glutathione and tyrosine phosphatases. J. Biol. Chem. *278*, 38360-38367.

Back, S.H., Scheuner, D., Han, J., Song, B., Ribick, M., Wang, J., Gildersleeve, R.D., Pennathur, S., and Kaufman, R.J. (2009). Translation attenuation through eIF2alpha phosphorylation prevents oxidative stress and maintains the differentiated state in beta cells. Cell Metab. *10*, 13-26.

Berasain, C. and Avila, M.A. (2014). The EGFR signalling system in the liver: from hepatoprotection to hepatocarcinogenesis. J. Gastroenterol. *49*, 9-23.

Brunet, A., Bonni, A., Zigmond, M.J., Lin, M.Z., Juo, P., Hu, L.S., Anderson, M.J., Arden, K.C., Blenis, J., and Greenberg, M.E. (1999). Akt promotes cell survival by phosphorylating and inhibiting a Forkhead transcription factor. Cell *96*, 857-868.

Carballo, M., Conde, M., El Bekay, R., Martin-Nieto, J., Camacho, M.J., Monteseirin, J., Conde, J., Bedoya, F.J., and Sobrino, F. (1999). Oxidative stress triggers STAT3 tyrosine phosphorylation and nuclear translocation in human lymphocytes. J. Biol. Chem. *274*, 17580-17586.

Carpenter, G. and Cohen, S. (1990). Epidermal growth factor. J. Biol. Chem. *265*, 7709-7712.

Chiarugi, P. and Buricchi, F. (2007). Protein tyrosine phosphorylation and reversible oxidation: two cross-talking posttranslation modifications. Antioxid. Redox Signal. *9*, 1-24.

Choi, W.G., Han, J., Kim, J.H., Kim, M.J., Park, J.W., Song, B., Cha, H.J., Choi, H.S., Chung, H.T., Lee, I.K., et al. (2017). eIF2alpha phosphorylation is

required to prevent hepatocyte death and liver fibrosis in mice challenged with a high fructose diet. Nutr. Metab. (Lond.) *14*, 48.

Chowdhry, S., Zhang, Y., McMahon, M., Sutherland, C., Cuadrado, A., and Hayes, J.D. (2013). Nrf2 is controlled by two distinct beta-TrCP recognition motifs in its Neh6 domain, one of which can be modulated by GSK-3 activity. Oncogene *32*, 3765-3781.

Citri, A. and Yarden, Y. (2006). EGF-ERBB signalling: towards the systems level. Nat. Rev. Mol. Cell Biol. *7*, 505-516.

Fan, Q.W., Cheng, C.K., Gustafson, W.C., Charron, E., Zipper, P., Wong, R.A., Chen, J., Lau, J., Knobbe-Thomsen, C., Weller, M., et al. (2013). EGFR phosphorylates tumor-derived EGFRvIII driving STAT3/5 and progression in glioblastoma. Cancer Cell *24*, 438-449.

Filosto, S., Khan, E.M., Tognon, E., Becker, C., Ashfaq, M., Ravid, T., and Goldkorn, T. (2011). EGF receptor exposed to oxidative stress acquires abnormal phosphorylation and aberrant activated conformation that impairs canonical dimerization. PLoS One *6*, e23240.

Gamou, S. and Shimizu, N. (1995). Hydrogen peroxide preferentially enhances the tyrosine phosphorylation of epidermal growth factor receptor. FEBS Lett. *357*, 161-164.

Goldkorn, T., Balaban, N., Matsukuma, K., Chea, V., Gould, R., Last, J., Chan, C., and Chavez, C. (1998). EGF-Receptor phosphorylation and signaling are targeted by H2O2 redox stress. Am. J. Respir. Cell Mol. Biol. *19*, 786-798.

Guren, T.K., Odegard, J., Abrahamsen, H., Thoresen, G.H., Susa, M., Andersson, Y., Ostby, E., and Christoffersen, T. (2003). EGF receptor-mediated, c-Src-dependent, activation of Stat5b is downregulated in mitogenically responsive hepatocytes. J. Cell. Physiol. *196*, 113-123.

Hagenbuchner, J., Kuznetsov, A., Hermann, M., Hausott, B., Obexer, P., and Ausserlechner, M.J. (2012). FOXO3-induced reactive oxygen species are regulated by BCL2L11 (Bim) and SESN3. J. Cell Sci. *125*, 1191-1203.

Han, J., Back, S.H., Hur, J., Lin, Y.H., Gildersleeve, R., Shan, J., Yuan, C.L., Krokowski, D., Wang, S., Hatzoglou, M., et al. (2013). ER-stress-induced transcriptional regulation increases protein synthesis leading to cell death. Nat. Cell Biol. *15*, 481-490.

Haouzi, D., Lekehal, M., Moreau, A., Moulis, C., Feldmann, G., Robin, M.A., Letteron, P., Fau, D., and Pessayre, D. (2000). Cytochrome P450-generated reactive metabolites cause mitochondrial permeability transition, caspase activation, and apoptosis in rat hepatocytes. Hepatology *32*, 303-311.

Heppner, D.E. and van der Vliet, A. (2016). Redox-dependent regulation of epidermal growth factor receptor signaling. Redox Biol. *8*, 24-27.

Jorissen, R.N., Walker, F., Pouliot, N., Garrett, T.P., Ward, C.W., and Burgess, A.W. (2003). Epidermal growth factor receptor: mechanisms of activation and signalling. Exp. Cell Res. *284*, 31-53.

Kim, D., Dai, J., Fai, L.Y., Yao, H., Son, Y.O., Wang, L., Pratheeshkumar, P., Kondo, K., Shi, X., and Zhang, Z. (2015). Constitutive activation of epidermal growth factor receptor promotes tumorigenesis of Cr(VI)-transformed cells through decreased reactive oxygen species and apoptosis resistance development. J. Biol. Chem. *290*, 2213-2224.

Kim, M.K., Yee, J., Cho, Y.S., Jang, H.W., Han, J.M., and Gwak, H.S. (2018). Risk factors for erlotinib-induced hepatotoxicity: a retrospective follow-up study. BMC Cancer *18*, 988.

Kitade, M., Factor, V.M., Andersen, J.B., Tomokuni, A., Kaji, K., Akita, H., Holczbauer, A., Seo, D., Marquardt, J.U., Conner, E.A., et al. (2013). Specific fate decisions in adult hepatic progenitor cells driven by MET and EGFR signaling. Genes Dev. *27*, 1706-1717.

Lee, S.R., Kwon, K.S., Kim, S.R., and Rhee, S.G. (1998). Reversible inactivation of protein-tyrosine phosphatase 1B in A431 cells stimulated with epidermal growth factor. J. Biol. Chem. *273*, 15366-15372.

Lewerenz, J. and Maher, P. (2009). Basal levels of eIF2alpha phosphorylation determine cellular antioxidant status by regulating ATF4 and xCT expression. J. Biol. Chem. *284*, 1106-1115.

Li, J., Zhao, M., He, P., Hidalgo, M., and Baker, S.D. (2007). Differential metabolism of gefitinib and erlotinib by human cytochrome P450 enzymes. Clin. Cancer Res. *13*, 3731-3737.

Liebmann, C. (2011). EGF receptor activation by GPCRs: an universal pathway reveals different versions. Mol. Cell. Endocrinol. *331*, 222-231.

Liu, L., Wise, D.R., Diehl, J.A., and Simon, M.C. (2008). Hypoxic reactive oxygen species regulate the integrated stress response and cell survival. J. Biol. Chem. *283*, 31153-31162.

Ma, Q. (2013). Role of nrf2 in oxidative stress and toxicity. Annu. Rev. Pharmacol. Toxicol. *53*, 401-426.

Miklossy, G., Hilliard, T.S., and Turkson, J. (2013). Therapeutic modulators of STAT signalling for human diseases. Nat. Rev. Drug Discov. *12*, 611-629.

Morita, M., Matsuzaki, H., Yamamoto, T., Fukami, Y., and Kikkawa, U. (2008). Epidermal growth factor receptor phosphorylates protein kinase C {delta} at Tyr332 to form a trimeric complex with p66Shc in the H2O2-stimulated cells. J. Biochem. *143*, 31-38.

Musallam, L., Ethier, C., Haddad, P.S., and Bilodeau, M. (2001). Role of EGF receptor tyrosine kinase activity in antiapoptotic effect of EGF on mouse hepatocytes. Am. J. Physiol. Gastrointest. Liver Physiol. *280*, G1360-G1369.

Oh, H.Y., Namkoong, S., Lee, S.J., Por, E., Kim, C.K., Billiar, T.R., Han, J.A., Ha, K.S., Chung, H.T., Kwon, Y.G., et al. (2006). Dexamethasone protects primary cultured hepatocytes from death receptor-mediated apoptosis by upregulation of cFLIP. Cell Death Differ. *13*, 512-523.

Orcutt, K.P., Parsons, A.D., Sibenaller, Z.A., Scarbrough, P.M., Zhu, Y., Sobhakumari, A., Wilke, W.W., Kalen, A.L., Goswami, P., Miller, F.J., Jr., et al. (2011). Erlotinib-mediated inhibition of EGFR signaling induces metabolic oxidative stress through NOX4. Cancer Res. *71*, 3932-3940.

Ostrowski, J., Woszczynski, M., Kowalczyk, P., Trzeciak, L., Hennig, E., and Bomsztyk, K. (2000). Treatment of mice with EGF and orthovanadate activates cytoplasmic and nuclear MAPK, p70S6k, and p90rsk in the liver. J. Hepatol. *32*, 965-974.

Paech, F., Bouitbir, J., and Krahenbuhl, S. (2017). Hepatocellular toxicity associated with tyrosine kinase inhibitors: mitochondrial damage and inhibition of glycolysis. Front. Pharmacol. *8*, 367.

Paulsen, C.E., Truong, T.H., Garcia, F.J., Homann, A., Gupta, V., Leonard, S.E., and Carroll, K.S. (2011). Peroxide-dependent sulfenylation of the EGFR catalytic site enhances kinase activity. Nat. Chem. Biol. *8*, 57-64.

Proud, C.G. (2005). eIF2 and the control of cell physiology. Semin. Cell Dev. Biol. *16*, 3-12.

Quesnelle, K.M., Boehm, A.L., and Grandis, J.R. (2007). STAT-mediated EGFR signaling in cancer. J. Cell. Biochem. *102*, 311-319.

Rajesh, K., Krishnamoorthy, J., Kazimierczak, U., Tenkerian, C., Papadakis, A.I., Wang, S., Huang, S., and Koromilas, A.E. (2015). Phosphorylation of the translation initiation factor eIF2alpha at serine 51 determines the cell fate decisions of Akt in response to oxidative stress. Cell Death Dis. *6*, e1591.

Rakhit, A., Pantze, M.P., Fettner, S., Jones, H.M., Charoin, J.E., Riek, M., Lum, B.L., and Hamilton, M. (2008). The effects of CYP3A4 inhibition on erlotinib pharmacokinetics: computer-based simulation (SimCYP) predicts in vivo metabolic inhibition. Eur. J. Clin. Pharmacol. *64*, 31-41.

Rodriguez-Fragoso, L., Melendez, K., Hudson, L.G., Lauer, F.T., and Burchiel, S.W. (2009). EGF-receptor phosphorylation and downstream signaling are activated by benzo[a]pyrene 3,6-quinone and benzo[a]pyrene 1,6-quinone in human mammary epithelial cells. Toxicol. Appl. Pharmacol. *235*, 321-328.

Sadidi, M., Lentz, S.I., and Feldman, E.L. (2009). Hydrogen peroxide-induced Akt phosphorylation regulates Bax activation. Biochimie *91*, 577-585.

Sato, K. (2013). Cellular functions regulated by phosphorylation of EGFR on Tyr845. Int. J. Mol. Sci. *14*, 10761-10790.

Schneider, M.R. and Wolf, E. (2009). The epidermal growth factor receptor

ligands at a glance. J. Cell. Physiol. *218*, 460-466.

Schreier, B., Rabe, S., Schneider, B., Bretschneider, M., Rupp, S., Ruhs, S., Neumann, J., Rueckschloss, U., Sibilia, M., Gotthardt, M., et al. (2013). Loss of epidermal growth factor receptor in vascular smooth muscle cells and cardiomyocytes causes arterial hypotension and cardiac hypertrophy. Hypertension *61*, 333-340.

Sham, D., Wesley, U.V., Hristova, M., and van der Vliet, A. (2013). ATP-mediated transactivation of the epidermal growth factor receptor in airway epithelial cells involves DUOX1-dependent oxidation of Src and ADAM17. PLoS One *8*, e54391.

Sonenberg, N. and Hinnebusch, A.G. (2009). Regulation of translation initiation in eukaryotes: mechanisms and biological targets. Cell *136*, 731-745.

Wang, X., McCullough, K.D., Franke, T.F., and Holbrook, N.J. (2000). Epidermal growth factor receptor-dependent Akt activation by oxidative stress enhances cell survival. J. Biol. Chem. *275*, 14624-14631.

Wang, X.T., McCullough, K.D., Wang, X.J., Carpenter, G., and Holbrook, N.J. (2001). Oxidative stress-induced phospholipase C-gamma 1 activation enhances cell survival. J. Biol. Chem. *276*, 28364-28371.

Wek, R.C., Jiang, H.Y., and Anthony, T.G. (2006). Coping with stress: eIF2 kinases and translational control. Biochem. Soc. Trans. *34*, 7-11.

Weng, M.S., Chang, J.H., Hung, W.Y., Yang, Y.C., and Chien, M.H. (2018). The interplay of reactive oxygen species and the epidermal growth factor receptor in tumor progression and drug resistance. J. Exp. Clin. Cancer Res. *37*, 61.